ARMY RESEARCH LABORATORY

High-speed Digital Color Imaging Pyrometry

by John M. Densmore, Matthew M. Biss, Kevin L. McNesby, and Barrie E. Homan

ARL-TR-5571 **August 2011**

NOTICES

Disclaimers

The findings in this report are not to be construed as an official Department of the Army position unless so designated by other authorized documents.

Citation of manufacturer's or trade names does not constitute an official endorsement or approval of the use thereof.

Destroy this report when it is no longer needed. Do not return it to the originator.

Army Research Laboratory
Aberdeen Proving Ground, MD 21005

ARL-TR-5571 **August 2011**

High-speed Digital Color Imaging Pyrometry

John M. Densmore, Matthew M. Biss, Kevin L. McNesby
And Barrie E. Homan
Weapons and Materials Research Directorate, ARL

REPORT DOCUMENTATION PAGE	Form Approved OMB No. 0704-0188

1. REPORT DATE *(DD-MM-YYYY)*	2. REPORT TYPE	3. DATES COVERED (From - To)
August 2011	Final	

4. TITLE AND SUBTITLE	5a. CONTRACT NUMBER
High-speed Digital Color Imaging Pyrometry	5b. GRANT NUMBER
	5c. PROGRAM ELEMENT NUMBER

6. AUTHOR(S)	5d. PROJECT NUMBER
John M. Densmore, Matthew M. Biss, Kevin L. McNesby, and Barrie E. Homan	5e. TASK NUMBER
	5f. WORK UNIT NUMBER

7. PERFORMING ORGANIZATION NAME(S) AND ADDRESS(ES)	8. PERFORMING ORGANIZATION REPORT NUMBER
U.S. Army Research Laboratory ATTN: RDRL-WML-B Aberdeen Proving Ground, MD 21005	ARL-TR-5571

9. SPONSORING/MONITORING AGENCY NAME(S) AND ADDRESS(ES)	10. SPONSOR/MONITOR'S ACRONYM(S)
	11. SPONSOR/MONITOR'S REPORT NUMBER(S)

12. DISTRIBUTION/AVAILABILITY STATEMENT

Approved for public release; distribution unlimited.

13. SUPPLEMENTARY NOTES

14. ABSTRACT

Temperature measurements of high-explosive and combustion processes are difficult to obtain due to the speed and environment of the events. To overcome these challenges, we have characterized and calibrated a digital high-speed color camera that may be used to measure the temperature of such events. A two-color ratio method is used to calculate a temperature using the color filter array raw image data and a graybody assumption. If the raw image data is not available, temperatures may be calculated from the processed images or movies, pending proper analysis of the digital color imaging pipeline. We analyze three transformations within the pipeline (demosaicing, white balance, and gamma-correction) to determine their effect on the calculated temperature. Using this technique with a Phantom color camera, we measured the temperature of exploded C-4 charges. The surface temperature of the resulting fireball was found to rapidly increase after detonation and subsequently decayed to a constant value of approximately 1980~K.

15. SUBJECT TERMS

Pyrometry, color camera

16. SECURITY CLASSIFICATION OF:			17. LIMITATION OF ABSTRACT	18. NUMBER OF PAGES	19a. NAME OF RESPONSIBLE PERSON
a. REPORT	b. ABSTRACT	c. THIS PAGE			John M. Densmore
UNCLASSIFIED	UNCLASSIFIED	UNCLASSIFIED	UU	20	19b. TELEPHONE NUMBER (*Include area code*) (410) 306-4949

Standard Form 298 (Rev. 8/98)
Prescribed by ANSI Std. Z39.18

Contents

List of Figures

Acknowledgments

This research was supported in part by an appointment to the U.S. Army Research Laboratory Postdoctoral Fellowship Program administered by the Oak Ridge Associated Universities and National Research Council through a contract with the U.S. Army Research Laboratory.

INTENTIONALLY LEFT BLANK.

1. Introduction

Temperature measurements of fast, destructive events (e.g., combustion, or high explosive detonations) presents many challenges. Conventional methods employing thermocouples, resistance temperature detectors, or diodes are intrusive and suffer from slow response times. Optical pyrometry is an alternative method that offers advantages over these conventional methods. Optical pyrometers are capable of operating at large standoff distances from the experiment, negating the potential for damage, and possess response times in the GHz range.

High speed optical pyrometry possessing high spatial and temporal resolution may be achieved with digital color imaging devices that use either charge couple devices (CCD) or complementary metal oxide semiconductor (CMOS) sensors. Infrared focal plane arrays with InSb photodiodes have been used to measure temperatures of in-flight slugs fired from rifles *(1)*. Visible spectrum optical pyrometers using CCD or CMOS sensors have been developed by a number of groups. T. Fu and coworkers have performed extensive work on the theory and optimization of color imaging pyrometers *(2–5)*. Pyrometers based on either CCD or CMOS color imaging devices have been used to measure soot temperature and concentrations *(6–8)*, laser weld temperatures *(9)*, and silicone carbide fibers *(10)*.

We characterized and calibrated a high speed Phantom Vision Research *(11)* color camera for use as an optical pyrometer. Complete calibration of the digital color camera is required for its use as a pyrometer. The two components that need to be characterized are the color filter array (CFA) sensitivity and an overall calibration factor. Raw gray-scale data from the CFA is used in conjunction with a physical model to determine the temperature of the imaged scene. The fundamental basis for the analysis assumes that the collected light is from a self-luminous object that behaves as a gray-body emitter. The analysis follows the two-wavelength ratio method *(12–13)*, extended to the broadband regime, using the light intensity collected from the CFA. Temperature calculations can be performed on movie or image files, if proper analysis of the color imaging pipeline is taken into account. The color image processing pipeline performs operations on the raw CFA data that could potentially introduce errors in the apparent temperature. Processing operations that may corrupt the data and cause an erroneous temperature are discussed in section 2.1.

2. Digital Color Imaging

Most high speed color cameras consist of a panchromatic complementary metal-oxide-semiconductor imaging sensor that is sensitive to light between 350-1100 nm. On top of the image sensor is a CFA that allows the production of color images. The CFA is a mosaic arrangement

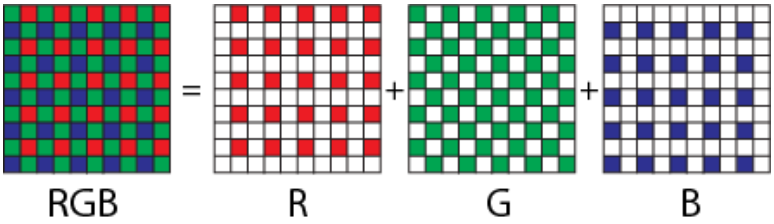

Figure 1. The Bayer color filter array *(15)*.

of color filters. In addition to the CFA, most cameras have an infrared (IR) cutoff filter to block radiation imperceptible to the human visual system.

Camera systems are designed to replicate a scene as seen by the human visual system. Each pigment or dye based color filter transmits a selected portion of the visible spectrum to the pixel beneath it. The spectral transmission of the color filters are designed to closely follow the color matching functions defined by the International Commission of Illumination (CIE), which describe the chromatic response of a standard observer's eye *(14)*. To ensure correct color reproduction, the color filters transmission should be a linear transformation of these color matching functions. This requirement, however, makes most camera filters non-ideal for use as a pyrometer. Nonetheless, it is not cost effective to design and build a camera with filters for temperature measurements.

The most common CFA used is the Bayer pattern *(*15). However, a number of other CFA patterns have been developed *(16–18)* and are used in commercial cameras. The Bayer pattern is composed of a 2×2 matrix with one red, one blue, and two green filters, figure 1. As the human visual system is more sensitive to the green region of the visible spectrum, there are twice as many green filters. As each pixel is sensitive to only one color channel, a demosaicing algorithm is necessary to recover a full color image consisting of red, green, and blue values for each pixel. This algorithm interpolates the two missing color values using adjacent pixel values in the raw CFA image.

Since each pixel has one color filter, the red, green, and blue color channels are sub-sampled across the image sensor. The sub-sampling introduces a nyquist frequency f_u. Spacial signals that have a frequency above f_u, are aliased and can not be fully interpolated. The aliasing of the color channels will cause errors in the color reproduction.

2.1 Image Processing

A generic outline of the steps taken to transform a raw gray-scale CFA image to a full color image is shown in figure 2. The steps that are of most importance for pyrometric measurements are CFA demosaicing, white balancing, and gamma-correction.

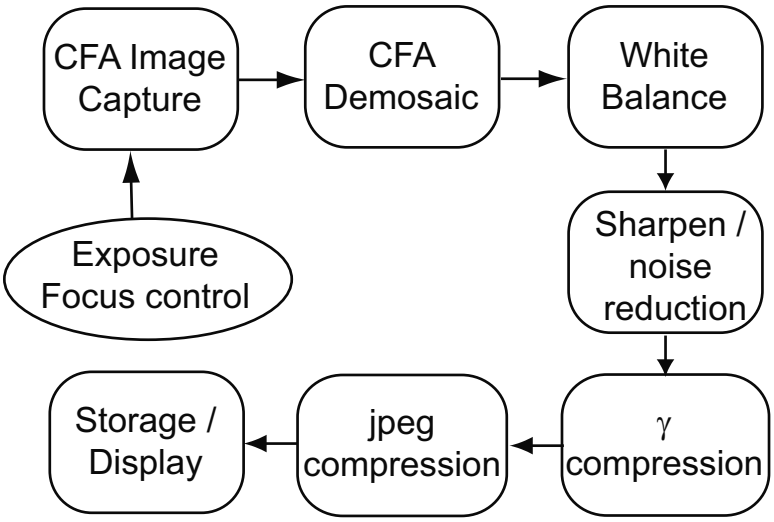

Figure 2. The color imaging processing pipeline. A generic outline of steps that must be taken to transform light collected by a lens to reproduce a full color image suitable for viewing *(19–24)*.

A full color image consists of pixels possessing three values that represent the red, green, and blue color channels. These three colors are combined to produce a color gamut. A demosaicing algorithm is used to create a full color image from the CFA image. Modern demosaicing algorithms may be nonlinear, and adaptive to the scene. Many are also proprietary to the camera manufacturer and therefore unpublished. Vision Research's Cine Viewer software offers six different demosaicing methods from "fastest" to "best". The quality and RGB values of an image change depending on what method is chosen. Different demosaicing methods can be found in references *(25–29)*.

The present research has developed a custom demosaicing algorithm to retain data fidelity. A $(n \times n)$ mean-interpolation scheme is used to reconstruct a full color image from the CFA image. For each pixel, the RGB values are calculated as the mean value from inside a $(n \times n)$ kernel; color values that are missing in the CFA are ignored in the mean value calculation. This calculation is modified near the edge of the image to only include elements within the image. In figure 3, a mean method is used to calculate the RGB values at pixel (3,3) which is described by the following,

$$G_{33} = \frac{1}{5}(G_{22} + G_{24} + G_{33} + G_{42} + G_{44}) \quad (1)$$

$$R_{33} = \frac{1}{2}(R_{32} + R_{34}) \quad (2)$$

$$B_{33} = \frac{1}{2}(B_{23} + B_{43}). \quad (3)$$

The $(n \times n)$ mean demosaicing method acts like a low-pass filter removing possible high frequency spatial signals that can not be measured by the CFA. As with all demosaicing

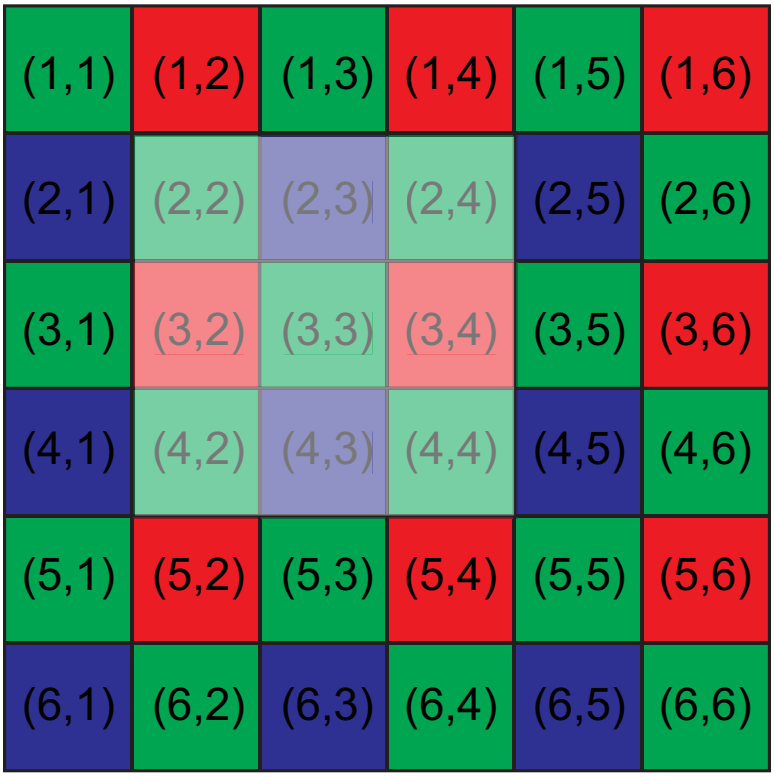

Figure 3. A Bayer CFA pattern with a (3×3) kernel used to calculate the mean values of the RGB channels at pixel (3,3).

methods, there is a downside: the edges inside the image are not handled well. As a result, smoothing and false coloring are introduced by the "zipper effect" textit (28, 29). These artifacts cause inaccurate color channel ratios along edges, ultimately resulting in erroneous temperature calculations at edges. While more advanced methods could be used to obtain correct colors, these methods rely on correlations between the RGB channels and should be avoided because the temperature calculation depends on the color channel ratio.

After the full color RGB image is obtained, white balancing is performed to correct for the spectral distribution, i.e., color temperature, of the illumination source, (figure 4) *(19)*. While the human visual system is capable of automatically adjusting to the illumination source color temperature, colors measured by image sensors depend on the illumination source. The measured color of a white object depends on the color temperature of the source. For example, a white object illuminated by a tungsten light (T_c=3000 K) appears reddish, under direct sunlight (T_c=5000 K) appears neutral, and under overcast conditions (T_c=9000 K) appears blueish. This is clearly an undesirable effect within consumer photography. The white point is defined by the source illuminant or by imaging a known neutral object if the illuminant is unknown. Once the white point is known, the RGB values are scaled by an appropriate value, R_w, G_w, and B_w

$$\begin{pmatrix} R_b \\ G_b \\ B_b \end{pmatrix} = \begin{pmatrix} 255/R_w & 0 & 0 \\ 0 & 255/G_w & 0 \\ 0 & 0 & 255/B_w \end{pmatrix} \begin{pmatrix} R_u \\ G_u \\ B_u \end{pmatrix}$$

where the u subscript is for the unbalanced raw data and the b subscript is for white balanced values. This correction ensures that white objects appear white in an image regardless of the illumination source. The fundamental assumption of the pyrometric analysis is that temperature calculations are performed only on self-luminous objects that behave as gray-body emitters. Since the temperature calculation depends on the spectral characteristic of the radiation, any adjustments to the RGB values would cause an error in the temperature. White balancing must be considered if analyzing processed movie or image files.

Charged coupled devices and CMOS imaging sensors are linear devices. Their pixel values are proportional to the exposure, where the exposure is a product of light intensity and count duration. But, since the human visual system is highly nonlinear with respect to exposure, most color spaces and storage formats have been designed with a gamma-correction (γ). The simplest γ-correction is a power-law that relates the photo-site voltage to the pixel value,

$$pixelvalue = V_{in}^{(1/\gamma)}. \tag{4}$$

When the image is viewed, the pixel values are decompressed by,

$$V_{out} = pixelvalue^{\gamma}. \tag{5}$$

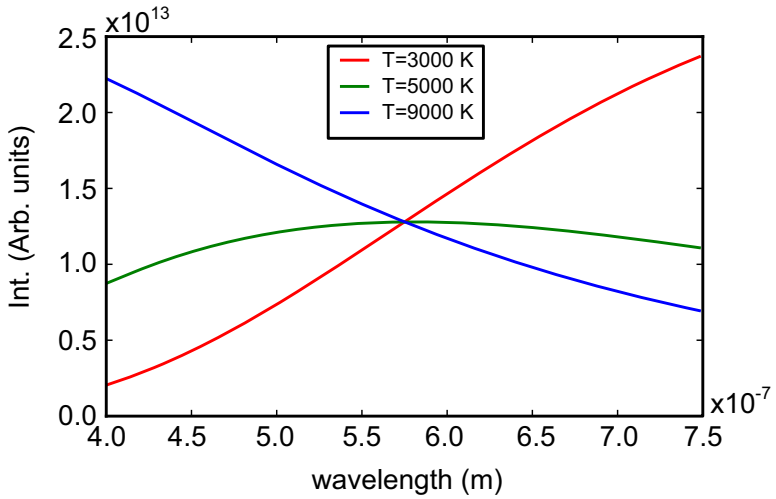

Figure 4. White balance is performed to correct for the spectral distribution of the source illuminate. A white object under a T_c=3000 K light will appear blue, T_c=5000 K will appear neutral, and T_c=9000 K will appear red. The intensity has been normalized at 575 nm.

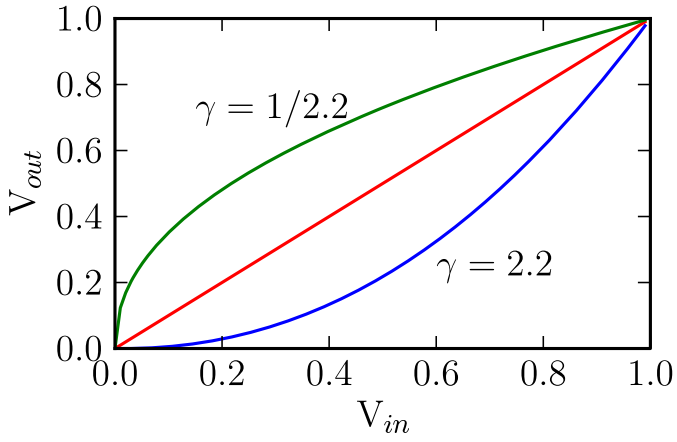

Figure 5. A power law gamma correction relating the voltage from the sensor (V_{in}) and the voltage out or pixel value (V_{out}).

The default gamma value for most camera systems is 2.2, which is also the gamma value for the common sRGB color space *(30)*.

Figure 5 shows a linear, γ-compressed, and decompressed curves. Darker regions correspond to small values of V_{in} and brighter regions correspond to large values of V_{in}. The γ-compressed curve expands the darker regions while the brighter regions are compressed. When the image is displayed, the pixel values are decompressed, and a linear relationship between the exposure and pixel value is regained. A considerable error in the temperature can occur if the γ-correction is not properly taken into account.

2.2 Physical Model

Blackbody radiation was first described by Planck in 1901 *(31)*. The spectral radiance of a blackbody depends only on the temperature T and wavelength λ,

$$L(\lambda, T) = \frac{C_1}{\lambda^5} \frac{\epsilon(\lambda, T)}{e^{C_2/T\lambda} - 1}, \tag{6}$$

where $C_1 = 37413 * 10^{-20}$ [W/m^2], $C_2 = 14388 * 10^{-6}$ [mK], and $\epsilon(\lambda, T)$ is the surface emissivity. For a blackbody, $\epsilon(\lambda, T) = 1$ in equation 3, whereas real objects have an emissivity of less than one. We assume that emissivity is constant over the visible region, a graybody assumption *(32)*.

A linear response model *(33)* was used to develop an analytical expression for the raw CFA values, equation 4 response D to an input spectral power density $S(\lambda)$ is

$$D = \Psi_i \Delta A_d \Delta \omega_d \Delta t \int \tau(\lambda) S(\lambda) \chi_i(\lambda) d\lambda, \tag{7}$$

where the index i is one of the color channels (red, green, or blue), Ψ_i is the gain of the internal electronics, $\chi_i(\lambda)$ is the spectral sensitivity of the color filter, $\tau(\lambda)$ is the transmission through the lens, ΔA_d is the area of the pixel, $\Delta \omega_d$ is the solid angle subtended by the pixel, and Δt is the exposure time. The integral range is over the visible region of the spectrum. We assume that the transmission through the lens is wavelength independent.

Since the absolute RGB value of each pixel is not calculable, a two-color ratio analysis is performed to calculate a temperature at each pixel *(13, 12)*. With equations 3 and 4, an expression for the ratio of two color channels can be calculated,

$$\frac{Green}{Red} = \frac{\Psi_g \int L(\lambda, T) \chi_g(\lambda) d\lambda}{\Psi_r \int L(\lambda, T) \chi_r(\lambda) d\lambda}. \tag{8}$$

For the temperature range of interest, the green and red channels are most appropriate as they provide the largest signal-to-noise value. However, the green/blue or red/blue ratio may be used if higher temperatures are expected. An overall calibration factor $C_{gr} = \Psi_g / \Psi_r$ is required because the absolute light intensity, lens optics, and internal camera electronics are unknown. This was measured by imaging a calibrated blackbody source, section 2.3.

2.3 Device Characterization

Since the dyes (pigments) used in the CFA are nonideal, their spectral transmittance must be known to calculate the analytical calibration curve, equation 5. There are several methods

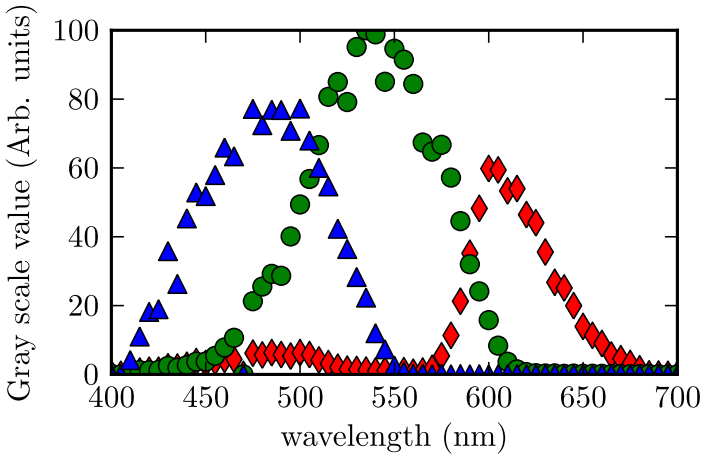

Figure 6. Spectral transmittance of the filters that compose the CFA. The data is in excellent agreement with the manufacture's data.

available to measure the spectral transmittance of color filters, see *(34, 34, 20)*. For this experiment, a monochromator, standard light source, photomultiplier tube (PMT), and color camera were used to measure the spectral response of the filters used in the color filter array. The output of the monochromator was imaged with the color camera and then measured with the PMT. Discrete measurements were made between 400 and 700 nm in 5 nm steps. The camera's response at pixels representing the different color filters $Q_i(\lambda)$ (i = red, green, and blue) is related to the measured PMT signal $P(\lambda)$ by,

$$Q_i(\lambda) = \chi_i(\lambda) * P(\lambda), \tag{9}$$

where $\chi_i(\lambda)$ is the spectral transmittance of the color filters. The manufacturer's published PMT sensitivity was used to correct the PMT signal. A singular value decomposition was used to solve the set of linear equations in equation 6. The measured spectral sensitivity of the filters used in the cameras CFA is shown in figure 6, and is in excellent agreement with the data provided by the camera's manufacturer *(36)*.

The overall calibration factor C_{gr} in equation 5 was measured with an Omega BB-4 blackbody source. The constant is independent of light intensity and constant at temperatures above 1100 K. The analytical curve and the measured blackbody data are shown in figure 7. At temperatures below 1100 K, the signal-to-noise increases significantly, as the maximum in the Planck curve moves to longer wavelengths of the infrared region and less light is emitted in the visible region.

2.4 Noise

A potential source of noise and non-linearity in the system is dark current, which is one of the largest sources of noise in digital imagers. Further sources of noise can be found

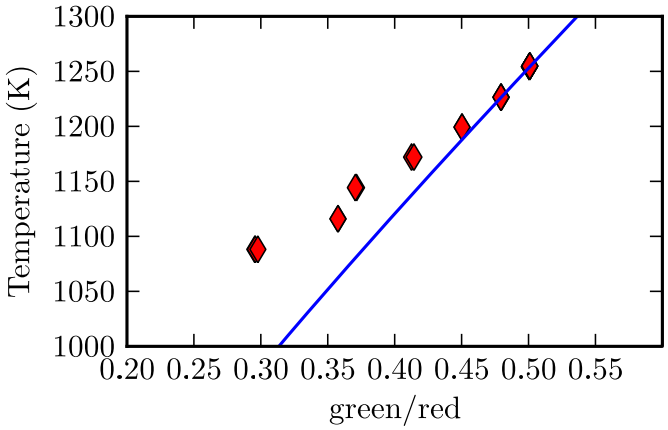

Figure 7. The analytical calibration curve equation 5 (blue curve) and measured data from a blackbody source, red triangles.

in reference *(19)*, but will not be discussed here. Dark current is generated by thermally excited electrons that accumulate at the photo-site. It has been shown that the dark current of a sensor depends on its temperature and the exposure duration *(37)*. Images taken at short exposure durations suffered from significant dark current noise. To correct for the dark current noise, a baseline image was taken with a cap covering the lens and was subtracted from the actual image. A baseline image was taken whenever the camera settings or ambient temperature changed.

3. Results - High Explosive Imaging

Detonated high explosives produce a rapidly expanding fireball of detonation products. If the explosive is underoxidized, the excess fuel burns with atmospheric oxygen (a process known as afterburning) *(38)*. Soot-like particles of unburned fuel or other solids account for the majority of the emitted light. These particles emit like a graybody which is described by Planck's law, equation 3 *(32)*. Since the surface of the fireball is optically thick, the light from the interior is not imaged by the camera.

The color camera pyrometer has been used to measure the surface temperature of centrally detonated spherical C-4 charges with a mass of 228 grams and suspended above a 1.5 square meter steel table. In addition to the color pyrometer, three other pyrometers were used to measure the temperature of the exploded charges. The full test results are reported in *(39)*.

Proper exposure setting is critical for obtaining temperature measurements of high explosives. Saturation and blooming occurs when the exposure time is too long, while an exposure time that is too short will cause the image to appear dark and possess a small signal-to-noise ratio. For all test shots, a 2 μs exposure was used with an f/22 35 mm lens. These settings provide images with sufficient light. The camera's maximum resolution is 1024×1024, however, the region of interest required a smaller area which increased the camera's maximum frame rate to 33,000 frames per second in some shots. The camera was operated in the circular buffer mode. In this mode, a set number of frames is recorded after the trigger pulse, with the remainder of the camera's memory filled by images before the trigger pulse. As a consequence, the start of an exposure is not synchronized to the start of the detonation. There is always a "jitter" of at least one frame in the absolute timing of the event. The surface temperature of an exploded charge is shown in figure 8. The surface temperature is relatively homogeneous with a variation of approximately 75 K. All measured charges showed similar temperature maps. A spectrograph was used to characterize any discreet emission or absorption. The only observable emission was from the sodium doublet at 589 nm. The strength of Na emission caused a 10 K error in the calculated temperature. There was no sign of significant gaseous emission in the wavelength region of interest.

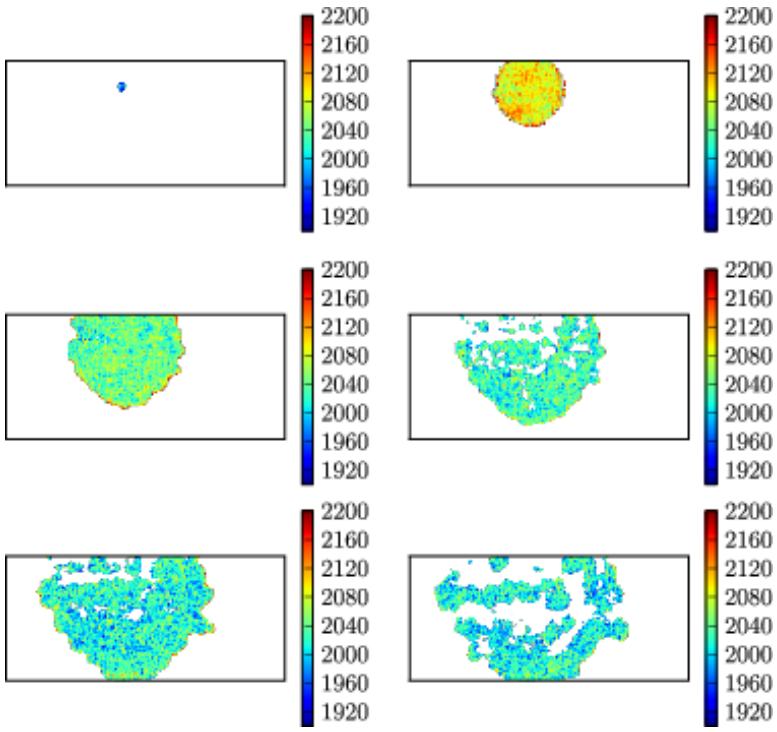

Figure 8. Surface temperature maps of exploded C-4 charges. The time between frames is 77 μs with a 2 μs exposure. The surface temperature is relatively homogeneous with a standard deviation of 75 K. The temperature is not calculated in the white regions because the light level was approximately the background value.

4. Conclusion

We have characterized and calibrated a high speed color camera that can be used as an optical pyrometer. Raw images from the camera's CFA provide the spectral resolution necessary to perform a two-color ratio analysis. If processed image or movie files are available for analysis, then proper accounting of the digital color imaging pipeline is mandatory for accurate temperature calculations. This technique has been used to measure the surface temperature of exploded C-4 charges with time resolution on the microsecond scale. Future work is planned to include a variable emissivity of sooting flames *(40–44)*.

References

[1] Richards, Austin A. Applications for High-speed Infrared Imaging.*26th International Congress on High-Speed Photography and Photonics* **2005**, *5580* (1), 137–145.

[2] Fu, T.; Cheng, X.; Shi, C.; Zhong, M.; Liu, T.; Zheng, X. The Set-up of a Vision Pyrometer. *Measurement Science and Technology* **2006**, *17*, 659–665.

[3] Fu, T.; Cheng, X.; Yang, Z. Theorical Evaluation of Measurement Uncertainties of Two0color Pyrometry Applied to Optical Diagnostics. *Applied Optics* **2008**, *47*, 61128.

[4] Fu, T.; Cheng, Xiaofang; Fan, Xueliang; Ding, Jinlei. The Analysis of Optimization Criteria for Multi-band Pyrometry. *Metrologia* **2004**, *41* (4), 305–313.

[5] Fu, T.; Cheng, Xiaofang; Zhong, Maohua; Liu, Tiemin. The Theoretical Prediction Analyses of the Measurement Range for Multi-band Pyrometry. *Measurement Science and Technology* **2006**, *17* (10), 2751–2756.

[6] Fu, T.; Wang, Zhe; Cheng, Xiaofang .Temperature Measurements of Diesel Fuel Combustion with Multicolor Pyrometry. *Journal of Heat Transfer* **2010**, *132* (5), 051602.

[7] Lu, H.; Ip, L.; Mackrory, A.; Werrett, L.; Scott, J.; Tree, D.; Baxter, L. Particle Surface Temperature Measurements with Multicolor Band Pyrometry. *AIChE* **2009**, *55* 243.

[8] Simonini, S.; Elston, S.; Stone, C. Soot Temperature and Concentration Measurements From Colour Charge Coupled Device Camera Images Using a Three-colour Method. *Proc Instn Mech Enger* **2001**, *215* 1041.

[9] Bardin, F.; McBride, R.; Moore, A.; Morgan, S.; Williams, S.; Jones, J.; Hand, D. Real Time Temperature Measurement for Process Monitoring of Laser Conduction Welding. In *Proceedings of the 23rd International Congress on Applications of lasers and electro-optics*, 20041.

[10] Maun, J. D.; Sunderland, P. B.; Urban, D. L. Thin-filament Pyrometry with a Digital Still Camera. *Applied Optics* **2007**, *46*, 483.

[11] Vision Research.*High Speed Cameras*. (accessed August 30, 2010). http://www.visionresearch.com/.

[12] DeWitt, D. P.; Nutter, Gene D. editors. *Theory and Practice of Radiation Thermometry*. John Wiley & Sons, 1988.

[13] Grum, Rhanc; Becjerer, Richad J. editors. *Optical Radiation Measurements*.Academic Press, 1979.

[14] CIE, *CIE - Internation Commission on Illumination*, 2010 (accessed September 20, 2010). http://cie.co.at/.

[15] Bayer, B. E. Color Imaging Array. U. S. Patent No. 3 971 065, 1976.

[16] Yamanaka, S. Solid State Color Cameras. U.S. Patent No. 4 054 906, 1977.

[17] Lukac, R.; Planiotis. Color Filter Arrays, Design and Performace Analysis. *IEEE Transactions on Consumer Electronics* **2005**, *51*, 1260–1267.

[18] Kijima, T.; Nakamura, H.; Compton, J.; Hamilton, J. Image sensore with improved light sensitivity. U.S. Patent No. 0 177 236, 2007.

[19] Nakamuri, Junichi, editor. *Image Sensors and Signal Processing for Digital Still Cameras*. CRC Press, 2006.

[20] Jahne, Bernd, editor. *Practical Handbook on Image Processing for Scientific and Technical Applications*. CRC Press, 2004.

[21] Russ, John C., editor. *The Image Processing Handbook, Fourth Edition*. CRC Press, 2002.

[22] Lukac, Rastislav; Plataniotos, Konstantinos, editors. *Color Image Processing: Methods and Applications*. CRC Press, 2006.

[23] Trussell, H. Joel; Saber, Eli; Vrhel, Michael. Color Image Processing. *IEEE Signal Processing Magazine* **Jan 2005**, 14.

[24] Ramaath, Rajeev; Synder, Wesley E. Yoo, Youngjun; Drew, Mark S.. Color Image Processing Pipeline. *IEEE Signal Processing Magazine* **Jan 2005**, 345.

[25] Ramaath, R.; Synder, W. E.; Bilbro, G. L. Sander, W. A. Demosaicking methods for bayer color arrays. *Journal of Electronic Imaging* **2002**, *11* (3), 306–315.

[26] Gunturk, B. K.; Glotzbach, J.; Altunbasak, Y.; Schafer, R .W.; Mersereau, R. M. Demosaicking: Color filter array interpolation. *IEEE Signal Processing Magazine* **Jan 2005**, 44.

[27] Lukac, R., editor. *Single-Sensor Imaging: Methods and Applications for Digital Cameras*. CRC Press, 2009.

[28] Adams, Jr., James E. Interactions Between Color Plane Interpolation and Other Image Processing Functions in Electronic Photography. *SPIE*, **1995**, *2416* 144–151

[29] Adams, Jr., James E. Design of Practical Color Filter Array Interpolation Algorithms for Digital Cameras. *SPIE*, **1997**, *3028*, 117–125.

[30] International Electrotechnical Commission. IEC, 1999 IEC 61966-2-1: Multimedia Systems and Equipment, Colour Measurements and Management, Part 2-1: Colour Management, Default RGB color space: sRGB, 1999.

[31] Planck, M. Ueber das gesetz der energieverteilung im normalspectrum. *Annalen der Physik*, 1901.

[32] Panagiotou, Thomai; Levendis, Yiannis; Delichatsios, Michael. Measurements of Particle Flame Temperatures Using Three-color Optical Pyrometry. *Combustion and Flame* **1996**, *104* (3), 272–287.

[33] Vora, P. L.; Farrell, J. E.; Tietz, J. D. Brainard, D. H. *Digital color cameras-1 response models*; Technical report, HPL-97-53 Hewlett-Packard Co., 1997.

[34] Finlayson, G. D.; Hordley, S.; Hubel, P. M. Recovering Device Sensitivities With Quadratic Programming. In *The Sixth Color Imaging Conference: Color Science, Systems and Applications*, page 90, 1995.

[35] Hubel, P. M.; Sherman, D.; Farrell, J. E. A Comparison of Methods for Sensor Spectral Sensitivity Estimation. In *IS&T and SID's 2nd Color Imaging Conference: Color Science,Systems and Applications* **1994**, *45*.

[36] Vision Research. private communications.

[37] Dunlap, J. C.; Bodegom, E.; Widenhorn, R. Correction of Dark Current in Consumer Cameras. *Journal of Electronic Imaging* **2010**, *19* (1). 013010.

[38] Cooper, P. W. *Explosive Engineering*. Wily-VCH, 1996.

[39] Densmore, J. M.; Biss, M. M.; McNesby, K. L.; Homan, B. E. Time Resolved Temperature Measurements of Suspended c-4 Spheres During and After Detonation. *To be submitted to ARL-TR*, 2010.

[40] Siddall, R. G.; McGrath, I. A. The Emissivity of Luminous Flames. In *Proceedings of the 9th Symposium (International) on Combustion*, p. 102, 1962.

[41] Pagni, P. J.; Bard S. Particulate Volume Fractions in Diffusion Flames. In *Proceedings of the 17th Symposium (International) on Combustion*, p. 1017, 1978.

[42] De Iuliis, S.; Barbini, M.; Benecchi, S.; Cignoli, F.; Zizak, G. Determination of the Soot Volume Fraction in an Ethylene Diffusion Flame by Multiwavelength Analysis of Soot Radiation. *Combustion and Flame* **1998**, *115*, 253.

[43] Matsui, Y.; Kamimoto, T.; Matsuoka, S. A Study on the Time and Space Resolved Measurement of Flame Temperature and Soot Concentration in a d.i. Diesel Engine by the Two-color Method. Technical Report 790491, SAE Tech. Paper, 1979.

[44] Quoc, H. X.; Vignon, J.-M.; Brun, M. A New Approach of the Two-color Method for Determining Local Instantaneous Soot Concentration and Temperature in a d.i. Diesel Combustion Chamber. Technical Report 910736, SAE Tech. Paper, 1991.

1 (PDF only) DEFENSE TECHNICAL INFORMATION CTR
DTIC OCA
8725 JOHN J KINGMAN RD
STE 0944
FORT BELVOIR VA 22060-6218

1 DIRECTOR
US ARMY RESEARCH LAB
IMNE ALC HRR
2800 POWDER MILL RD
ADELPHI MD 20783-1197

1 DIRECTOR
US ARMY RESEARCH LAB
RDRL CIO LL
2800 POWDER MILL RD
ADELPHI MD 20783-1197

1 DIRECTOR
US ARMY RESEARCH LAB
RDRL CIO MT
2800 POWDER MILL RD
ADELPHI MD 20783-1197

1 DIRECTOR
US ARMY RESEARCH LAB
RDRL D
2800 POWDER MILL RD
ADELPHI MD 20783-1197

1 DIR BENET WEAPONS LAB
TECH LIB
WATERVLIET NY 12189-4000

1 CDR NAVAL RSRCH LAB
TECH LIB
WASHINGTON DC 20375-1972

2 OFFICE OF NAVAL RSRCH
C BEDFORD
B ALMQUIST
875 N RANDOLPH ST RM 653
ARLINGTON VA 22203-1927

ABERDEEN PROVING GROUND

6 DIR USARL
RDRL WML
M ZOLTOWSKI
RDRL WML B
J MORRIS
B E HOMAN
J M DENSMORE
RDRL WML C
K L MCNESBY
B ROOS

INTENTIONALLY LEFT BLANK.